AIP | Applied Physics Letters

Strain-induced stabilization of Al functionalization in graphene oxide nanosheet for enhanced NH3 storage

Yunguo Li, Abir De Sarkar, Biswarup Pathak, and Rajeev Ahuja

Citation: Appl. Phys. Lett. **102**, 243905 (2013); doi: 10.1063/1.4811494
View online: http://dx.doi.org/10.1063/1.4811494
View Table of Contents: http://apl.aip.org/resource/1/APPLAB/v102/i24
Published by the AIP Publishing LLC.

Strain-induced stabilization of Al functionalization in graphene oxide nanosheet for enhanced NH_3 storage

Yunguo Li,[1] Abir De Sarkar,[1,2,a)] Biswarup Pathak,[3] and Rajeev Ahuja[1,4]
[1]*Applied Materials Physics, Department of Materials Science and Engineering, Royal Institute of Technology (KTH), S-100 44 Stockholm, Sweden*
[2]*Department of Physics, Central University of Rajasthan, NH-8, Bandarsindri, Rajasthan 305801, India*
[3]*Department of Chemistry, Indian Institute of Technology, Indore 452017, India*
[4]*Condensed Matter Theory Group, Department of Physics and Astronomy, Box 516, Uppsala University, S-75120 Uppsala, Sweden*

(Received 10 July 2012; accepted 4 June 2013; published online 19 June 2013)

Strain effects on the stabilization of Al ad-atom on graphene oxide (GO) nanosheet as well as its implications for NH_3 storage have been investigated using first-principles calculations. Tensile strain is found to be very effective in stabilizing the Al ad-atom on GO. It strengthens the C–O bonds through an enhanced charge transfer from C to O atoms. Interestingly, Al's stability is governed by the bond strength of C-O rather than that of Al-O. Optimally strained Al-functionalized GO binds up to 6 NH_3 molecules, while it binds no NH_3 molecule in unstrained condition. © *2013 AIP Publishing LLC*. [http://dx.doi.org/10.1063/1.4811494]

Carbon nanostructures are very promising candidates for multifarious applications in nanoscience and nanotechnology, due to their light weight, low cost, and high surface to volume ratio.[1–8] However, carbon nanostructures are chemically inert in their pristine form, as gas molecules bind very loosely to them. This precludes most of its practical applications. Decorating or functionalizing these nanostructures with metal atoms are common and practical avenues to enhance their gas adsorption capacities,[5,7,9–11] which is brought about by the strong Lewis acid-base interaction between metal atoms and gas molecules.[1,4,12,13] Functionalization enables myriad potential applications of carbon nanostructures, including catalysis, molecular sensors, nanotechnology, biotechnology, energy storage, and biomedicine.[1,14–17] For a maximal utility of the functionalization, it needs to meet these two ends concurrently: (1) the binding of the dopant to the nanomaterial needs to be stable and (2) the functionalization is intended to be as effective as possible.[17] Weak binding of metal atoms to the substrates is still frequently encountered,[14,15,18] which brings down the utility of the functionalization. Several pathways have been explored to circumvent this problem, among which the employment of mechanical strain is found to be most economic and practical.[6,19,20] Strain occurs naturally at the interfaces of nanomaterials that differ in their lattice constants, for instance, in the growth of Ge thin films on Si substrate. Besides, strain is applied in nano-electromechanical systems (NEMS) and nano-optomechanical systems (NOMS) to tune the electronic and optical properties of nanomaterials. Up to 15% mechanical tensile strain has been experimentally realized in graphene.[21,22] Ten percent tensile strain has been found to significantly enhance the binding of metal ad-atoms to graphene and in turn, the adsorption strength of the gas molecules on the metal ad-atoms. Zhou *et al.*[6] have subjected metal-decorated graphene to mechanical strain, which not only stabilized the metal ad-atoms and counteracted their clustering propensity but also considerably enhanced their hydrogen storage capacity.

Shevlin and Guo[19] introduced defects in carbon substrates via vacancy creation to anchor metal dopants, while Zhou *et al.*[23] have demonstrated an improvement in H_2 molecular adsorption on a polarizable substrate by the application of electric field. Kim *et al.*[20] and Liu and Zeng[24] have resorted to substitutional doping of boron to facilitate a stronger binding of metal ad-atoms on carbon substrates. A large number of studies on stabilizing the functionalization of metal atoms on carbon nanostructures have advanced its scientific understanding. Yet, it still continues to be an ongoing issue, underscoring the need for a much deeper understanding and insight.

Among the metal functionalized carbon nanostructures, metal-decorated graphene oxide (GO) materials have been increasingly gaining popularity for its superior electronic properties, high surface to volume ratio, and low cost.[7,25–31] Actually, GO was already synthesized using a simple procedure way back in 1958.[32] In this article, we have explored the potential of Al-decorated GO (GO:Al) as a NH_3 storage material, as Al-doped carbon nanostructures have been found to bind gas molecules strongly.[33] Moreover, Al-functionalized GO has not yet been reported.

The incorporation of Al ad-atom into the GO is accompanied by a large number of structural changes, including C–O bond breaking and Al–O bond making. It is the purpose of this article to probe into the microscopic mechanism behind the strain-induced stabilization of Al ad-atom in the GO using first principles density functional theory and its implications for a more efficient storage of NH_3 molecules.

All calculations have been performed using the *ab initio* density functional theory as implemented in the Vienna *ab initio* simulation package (VASP).[34] The Perdew-Burke-Ernzerhof (PBE)[35] variant of the generalized gradient approximation (GGA-PBE) has been used for the exchange and correlation functional within the projector-augmented wave (PAW)[36] framework. The system is modeled as a 3×4 supercell of graphene (24 C atoms). A vacuum thickness of

a)Author to whom correspondence should be addressed. Electronic mail: abirdesarkar@gmail.com

16 Å in the direction normal to the surface was used to decouple the periodic images. A $4 \times 3 \times 1$ Monkhorst-Pack[37] k-mesh was used to sample the Brillouin zone. An energy cut off of 700 eV was used for the expansion of plane-wave basis. Atomic positions were optimized until the maximum force on each atom reached less than 0.001 a.u. All calculations were performed at 0 K.

First of all, we have ascertained the optimum position of the Al ad-atom on GO by geometry optimization calculations. Fig. 1(a) shows the supercell containing 24 carbon atoms and two epoxy oxygen atoms. According to the previous studies on GO nanosheet, the most stable positions for oxygen atoms in GO are the bridge sites of two adjacent carbon atoms. The most stable proposed structure of GO sheet with only epoxy functional units is that the epoxies are arranged in a line but at a distance of 3 C–C bond length on both sides of the graphene sheet.[7,26] So, we optimized the structure of GO with two epoxies as is shown in Figs. 1(a) and 1(b). The C–O distance is found to be 1.47 Å, and the bonds between functionalized carbon atoms lengthened from 1.42 Å (the C–C bond length in graphene) to 1.48 Å, which corresponds well with the previous reports.[7,25] The charge on the O atom is found to be −0.82e. O being more electronegative than C draws electronic charge towards itself. Then, we placed an Al atom at the center of the two epoxies at a distance of 2.00 Å from the epoxy O atoms. Figs. 1(c) and 1(d) show the stable structure obtained from the optimization calculations, in which the oxygen atoms cleave their bonds with one of the carbon atoms and strike a strong bond with the decorated Al atom. The C–O bond length increases to 1.49 Å, while the Al–O bond reaches 1.75 Å. Two valence electrons of the Al ad-atom are transferred to the two O atoms on its either side. As a result, the electronic charge on Al ad-atom and O atom reaches +2.00e and −1.5e, respectively. The O atoms gain the balance of −0.5e electronic charge from the C atoms of the underlying nanosheet.

The adsorption energy of an Al ad-atom on the GO nanosheet is calculated as

$$E_{BE} = (E_{GO} + E_{Al}) - E_{(GO:Al)}, \quad (1)$$

where E_{GO} is the total energy of GO before adsorbing an Al atom on it, E_{Al} is the total energy of a single Al atom in a unit cell of $10 \times 10 \times 10$ Å^3 dimensions, and $E_{(GO:Al)}$ is the total energy of relaxed GO:Al. The adsorption energy comes out to be 5.20 eV, which is much higher than that of Al_2 dimer in vacuum (1.62 eV), cohesive energy of Al in its bulk (3.39 eV/atom)[38] and the adsorption energy of a single Al ad-atom on graphene sheet (1.05 eV), thereby ruling out the possibility for clustering of Al ad-atoms.

In GO:Al nanosheet, each Al ad-atom is linked to the underlying nanosheet via two O atoms. Prior to decoration, these two O atoms were located at their respective epoxy positions, bonded to two underlying C atoms of the nanosheet. In the decorating process, the Al ad-atom bonds to the two epoxy O atoms on its either side. As a result, each of these two epoxy O atoms snaps one of their O–C bonds. The O–C bonds that survived the process of Al-doping were slightly weakened as indicated by the increase in O–C bond length. This is supported by experimental evidences[39] that Al is a good reducing agent for GO.

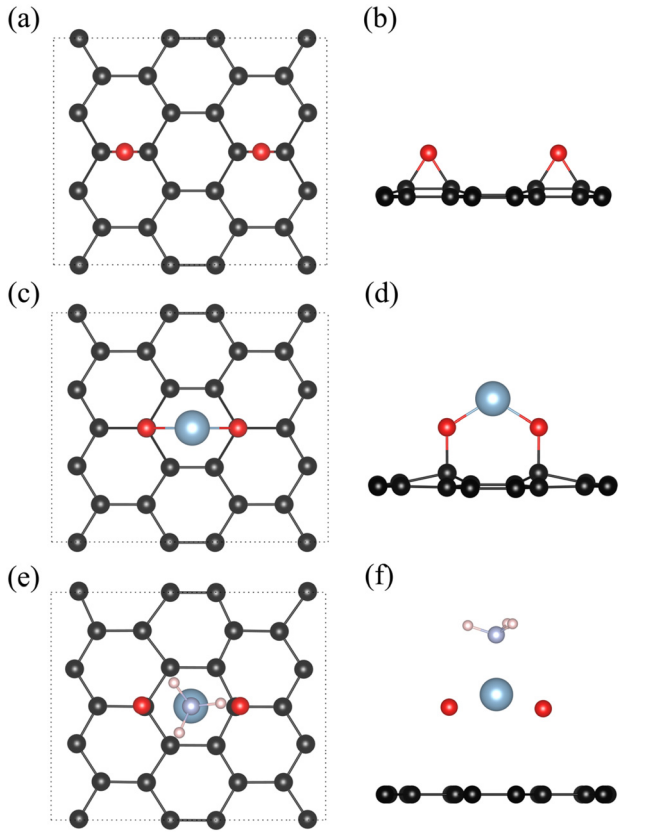

FIG. 1. (a) Top view of GO; (b) side view of GO; (c) top view of Al-decorated GO; (d) side view of Al-decorated GO; (e) top view of one NH_3 molecule on Al-decorated GO; (f) side view of one NH_3 molecule on Al-decorated GO.

The Al ad-atom binds to the GO nanosheet via two O–Al bonds. We have calculated the binding energy of Al to GO by providing different inputs for E_{GO} and E_{Al} in Eq. (1). The total energy of the GO part of GO:Al enters into E_{GO}, which is obtained through a static calculation after having removed the Al atom from the supercell, whereas E_{Al} is considered as the total energy of Al part of GO:Al and is calculated similarly after having removed GO from the supercell. The binding energy of Al to GO calculated in this way comes out to be 7.36 eV. Since an Al ad-atom is symmetrically bonded to 2 O atoms on its either side, bond energy of each O–Al bond is half of 7.36 eV, i.e., 3.68 eV. This method of calculating the binding energy of Al (or the bond energy of O-Al) is free from the effects of structural distortion or changes, which has otherwise been considered in the estimation of adsorption energy.

The Al ad-atom binds strongly to the O atoms of GO, which shows up in its high binding energy. The strong binding of the Al atom to the O atoms adversely affects the strength of the bonds of the O atoms with the underlying C atoms (designated as C1) of the substrate. From the perspective of bond order conservation, the strong O–Al bonds significantly weaken the bonds of the O atoms with the C atoms of substrate. Since the Al ad-atom is linked to the GO nanosheet via O atoms, the binding of O atoms to the substrate deserves a careful consideration under different set of conditions. The O–C bond strength/energy calculated in the way similar to that of the O–Al bond energy turns out to be 1.71 eV.

The GO:Al has been investigated for the purpose of NH_3 storage. First, we have used GO:Al for the adsorption

of one NH_3 molecule, using different distances between the Al ad-atom and the NH_3 molecules as well as different orientations of the molecules as starting points for geometry optimizations. Unfortunately, when a single NH_3 molecule interacts with the GO:Al, the NH_3 molecule is pulled to the Al ad-atom and the aforementioned O-Al-O functional unit rips off the substrate sheet, as shown in Figs. 1(e) and 1(f). It indicates that the adsorption of NH_3 further weakens the already weak O–C bonds, due to some bond order conservation. The O–C bonds are weakened to such an extent upon adsorption of a NH_3 molecule that the O-Al-O functional unit shown in Figs. 1(c) and 1(d) dissociates itself from the underlying substrate sheet. Here, the situation is different from that of Al-decorated graphene sheet in the sense that the Al ad-atom is indirectly linked to the substrate via the O atoms of the oxide. The striking features in GO:Al are the weak O–C bonds. Actually, the GO:Al may be looked upon as a graphene sheet decorated with the O-Al-O functional unit.

The tensile strain, varying from 0% to 15%, was applied along both arm-chair (x-axis) and zig-zag (y-axis) directions. The atomic positions were then relaxed in the strained structures. The GO:Al was found to be stable up to 10% tensile strain along the arm-chair direction and simultaneously up to 15% along the zig-zag direction. The structure of the Al-decorated GO collapses when the applied strain exceeds this range. So, we find the tolerance limit of GO:Al to tensile strain to be 10% along the arm-chair direction and 15% along the zig-zag direction.

An energetic analysis of the strain effects is not sufficient to reveal the underlying mechanism, as it involves a large number of changes in bond lengths in the system when it is subject to strain. In addition, we need to examine the strain-induced changes in the electronic structure and geometry of the O-Al-O functional unit. It is instructive to track the evolution in the binding of the O-Al-O functional unit to the underlying substrate under the application of mechanical strain.

Tensile strain induced effects show up more prominently through charge redistribution among the Al, O, and C atoms than through changes in the bond lengths. The maximum changes in O–C and O–Al bond lengths are found to be 0.077 Å and 0.014 Å, respectively, for the range of strain investigated in our work. Tensile strain on GO:Al is found to shorten the bond length of O-C, while it lengthens the O–Al bond. Furthermore, strain along the armchair direction is found to be more effectual than along the zig-zag direction in strengthening the C–O bonds. So, the applied tensile strain is found to be very effective in stabilizing the Al ad-atom on GO by strengthening the O–C bonds, while simultaneously reducing the O–Al bonds by a relatively much smaller magnitude.

To further elucidate the electronic mechanism behind strain induced stabilization of Al ad-atom, a Bader analysis of atomic charges was also performed. The charges on Al, O, and the C (C1 carbon atom) bonded to O are shown in Tables I–III, respectively. Under the application of tensile strain, O gained charge mainly from C and marginally from Al, which is consistent with the changes in bond length. The applied tensile strain is found to redistribute electronic charge among the Al, O, and the C1 atoms and thereby stabilize the functionalization of GO by Al. The O–C bond is strengthened by a significant charge transfer from C to O. In Table IV, the bond strength/energy of O–C bond shows a systematic increase with strain, and it maximizes to 2.84 eV at an optimally applied tensile strain (i.e., 5% strain along armchair direction and 15% along zigzag direction). The bond strength/energy of Al–O bond changes from 3.68 eV, corresponding to the strain free case, to 3.65 eV under

TABLE I. Electronic charge on Al ad-atom as a function of tensile strain applied along the two directions (X-axis: arm-chair, Y-axis: zig-zag).

	Strain along X-axis (%)			
Strain along Y-axis (%)	0	2.5	5.0	10
0	+2.00	+1.99	+2.00	+2.06
2.5	+2.01	+2.07	+2.08	+2.07
5.0	+2.03	+2.08	+2.08	+2.07
10	+2.08	+2.09	+2.09	+2.08
15	+2.09	+2.09	+2.10	…[a]

[a]The structure has collapsed at this pair of strain values.

TABLE II. Electronic charge on O atom as a function of tensile strain applied along the two directions (X-axis: arm-chair, Y-axis: zig-zag).

	Strain along X-axis (%)			
Strain along Y-axis (%)	0.0	2.5	5.0	10
0	−1.52	−1.69	−1.72	−1.77
2.5	−1.74	−1.77	−1.8	−1.89
5.0	−1.76	−1.79	−1.84	−1.89
10	−1.83	−1.88	−1.93	−2.03
15	−1.94	−1.97	−2.04	…[a]

[a]The structure has collapsed at this pair of strain values.

TABLE III. Electronic charge on one of the carbon atoms in the graphene sheet bonded to O under tensile strain applied along the two directions (X-axis: arm-chair, Y-axis: zig-zag). This carbon atom is designated as C1 atom in the text of the article.

	Strain along X-axis (%)			
Strain along Y-axis (%)	0.0	2.5	5.0	10
0.0	+0.49	+0.68	+0.70	+0.75
2.5	+0.73	+0.42	+0.78	+0.92
5.0	+0.76	+0.43	+0.84	+0.92
10	+0.82	+0.87	+0.93	+1.05
15	+0.95	+1.00	+1.08	…[a]

[a]The structure has collapsed at this pair of strain values.

TABLE IV. Bond strength/energy (in eV) of the O–C bond in Al-decorated GO under tensile strain applied along the two directions (X-axis: arm-chair, Y-axis: zig-zag).

	Strain along X-axis (%)			
Strain along Y-axis (%)	0	2.5	5.0	10
0	1.71	1.65	1.64	1.80
2.5	1.73	1.81	1.91	2.20
5.0	1.83	1.91	2.02	2.32
10	2.14	2.30	2.36	2.70
15	2.46	2.72	2.84	…[a]

[a]The structure has collapsed at this pair of strain values.

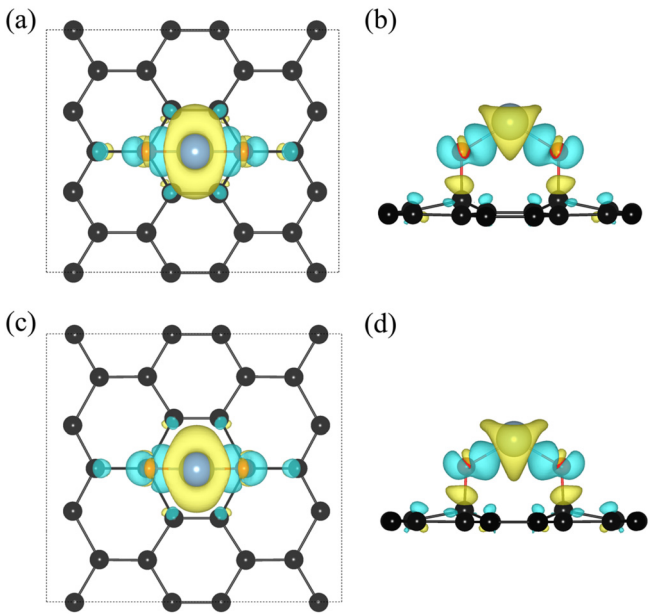

FIG. 2. Differential charge density plots (yellow: charge depletion, cyan: charge accumulation): (a) top view of unstrained Al-decorated GO; (b) side view of unstrained Al-decorated GO; (c) top view of optimally strained Al-decorated GO; (d) side view of optimally strained Al-decorated GO.

optimally applied tensile strain. As a result, the difference in electronic charge on Al ad-atom between these two cases is minimal: It does not change by more than 0.1 unit. The binding energy (BE) of an Al ad-atom is found to be almost insensitive to the application of strain. Therefore, strain induced stabilization of Al ad-atom on GO nanosheet is not reflected in the binding energy. Moreover, the adsorption energy of an Al ad-atom on GO (AE) shows an overall decreasing trend with the application of mechanical strain, as shown in Table V, implying a strain induced destabilization of Al functionalization in GO. This variation in the AE with strain is clearly found to be at odds with the systematic analysis of electronic structure based on bond lengths and atomic charge redistribution.

The optimal strain is found to be 5% along the armchair direction and 15% along the zig-zag direction, where the O–C bond strength reached its peak, as can be seen in Table IV. Fig. 2 shows the iso-surfaces for the differential electronic charge density on both unstrained and optimally strained GO:Al nanosheet. Figs. 2(a) and 2(b) correspond to the top and side view of the unstrained case, while Figs. 2(c) and 2(d) to the top and side view of the optimally strained case. The differential charge density is obtained from

$$\Delta\rho = \Delta\rho_{(GO:Al)} - (\Delta\rho_{Al} + \Delta\rho_{GO}), \tag{2}$$

where $\Delta\rho_{(GO:Al)}$, $\Delta\rho_{Al}$, and $\Delta\rho_{GO}$ denote the charge densities of the relaxed GO:Al, Al atom, and GO, respectively. Accumulation and depletion of charge around O and C, respectively, are found to occur in significant proportions under the application of strain, while charge around Al depletes marginally under strain. It indicates that charge redistributes mainly in the carbon and oxygen atoms of the GO nanosheet, while the electronic charge on Al dopant is not found to be significantly affected by the application of strain. This is also substantiated by the differential charge density plots.

Thereafter, we have examined the adsorption of NH_3 molecules on the optimally strained GO:Al nanosheet. Different distances between Al dopant and NH_3 molecules as well as different orientations of the molecules were used as starting points for geometry optimizations. The adsorption energy of NH_3 molecules and corresponding adsorbed structures are shown in Fig. 3. For a more accurate and a proper treatment of the weak van der Waals' (vdW) attractive forces which bind the NH_3 molecules to the optimally strained GO:Al, we have considered the van der Waals' dispersion interactions incorporated into GGA-PBE based on the semi-empirical correction of Grimme,[40] as implemented in VASP, for the calculation of the binding energies of NH_3.

To investigate the energetics of NH_3 adsorption, the adsorption energy of NH_3 was calculated as

$$E_{ads,NH_3} = \frac{E_{GO:Al} + nE_{NH_3} - E_{GO:Al-NH_3}}{n}, \tag{3}$$

where n refers to the number of adsorbed NH_3 molecules, $E_{GO:Al}$ to the total energy of relaxed GO:Al. E_{NH_3} is the total energy of a relaxed free NH_3 molecule, while $E_{GO:Al-NH_3}$ is the total energy of GO:Al with adsorbed NH_3 molecule(s).

Al ad-atom binds the first NH_3 molecule with a significant decrease in the total energy of the system (1.25 eV by GGA), with the NH_3 molecule lying on one side of the plane of the O-Al-O functional unit. It is justified since Al loses considerable charge along the direction normal to the plane of the O-Al-O functional unit. The distance between Al and

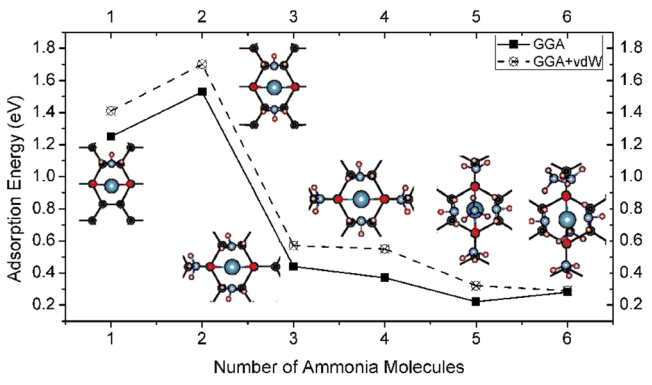

FIG. 3. Binding/adsorption energy of NH_3 molecule(s) in eV on optimally strained Al-decorated GO.

TABLE V. Adsorption energy (AE) of the Al ad-atom on the GO nanosheet (in eV) under tensile strain applied along the two directions (X-axis: armchair, Y-axis: zig-zag).

	Strain along X-axis (%)			
Strain along Y-axis (%)	0	2.5	5.0	10
0	5.20	5.06	4.91	4.45
2.5	3.20	4.42	4.22	1.46
5.0	2.93	4.3	4.11	1.54
10	2.67	4.07	3.93	1.85
15	0.63	3.86	3.78	…[a]

[a]The structure has collapsed at this pair of strain values.

N atom (d_{Al-N}) is 2.04 Å, while the O–Al and O–C bond lengths are 1.77 Å and 1.40 Å, respectively. The O–Al and O–C bond lengths remain almost unchanged upon adsorption, suggesting the stability of the O-Al-O functional unit against gas adsorption. The adsorption energy of the 2nd NH_3 molecule is 1.53 eV by GGA, suggesting a strong adsorption for the 2nd molecule as well. The two NH_3 molecules distributed themselves symmetrically on the two sides of the O-Al-O functional unit: d_{Al-N} is found to be 2.00 Å for the adsorption of the first 2 NH_3 molecules. The O–C bond length increased from 1.40 Å to 1.43 Å, but the O-Al distance decreased to 1.72 Å upon adsorption of the 2nd NH_3 molecule. It indicates that adsorption of the 2nd molecule weakens the O–C bonds slightly and at the same time, it strengthens the O–Al bonds a little. For the 3rd and the 4th molecule, the adsorption energies are found to be 0.44 eV and 0.37 eV by GGA, and the d_{Al-N} are 3.49 Å and 3.56 Å, and the adsorption energies of the 5th and 6th molecules are 0.22 eV and 0.28 eV, respectively. The O–C and O–Al bond lengths remain unchanged upon the adsorption of 3 to 6 NH_3 molecules. This shows that the adsorption of the molecules in succession hardly affects these two bonds. In Fig. 3, it can be observed that the results of vdW-GGA are consistent with that of GGA. Both these functionals give a similar trend in binding energies which converge when 6 NH_3 molecules physisorb on it. Due to a more accurate description of vdW interaction in vdW-GGA, it gives higher binding energies than GGA, as expected. Besides, the d_{Al-N} is found to vary slightly with the exchange correlation (XC) functionals. The d_{Al-N} for the first two adsorbed NH_3 molecules is found to be almost the same for both the XC functionals (i.e., GGA and vdW-GGA), while the d_{Al-N} is 0.2 Å shorter for the 4th molecule in calculations using vdW-GGA. For the 6th molecule, it is 0.3 Å shorter in vdW-GGA than in GGA. So, vdW-GGA enables Al to draw the 4th and the 6th NH_3 molecules a bit closer to itself.

So, the adsorption of six NH_3 molecules is found to be attainable, and the adsorption energies are found to lie within a reasonable range. More importantly, the adsorption of NH_3 molecules has not been found to produce any discernible effect on the structure of the O-Al-O functional unit. Therefore, the applied strain is found to be very efficacious in stabilizing the structure, suiting it for NH_3 adsorption and storage.

In summary, using first-principles calculations, we have studied the strain effects on the stabilization of the O-Al-O functional unit on GO:Al for NH_3 storage. The structural instability of Al on GO is clearly at variance with the high binding energy of Al on GO. Therefore, it was found necessary to assess the stability both from energetic and structural perspectives. The applied mechanical strain is found to effectively stabilize Al functionalization on GO, by tuning the charge redistribution among Al atom, O atom, and the underlying graphene sheet. Tensile strain strengthens the C–O bonds; while it simultaneously weakens the O–Al bonds marginally due to bond order conservation. The strength of the C–O bonds is found to underlie Al's stability in GO. While the unstrained GO:Al nanosheet is unable to bind even a single NH_3 molecule, it is found to bind up to six NH_3 molecules with considerably good binding energies when it is strained optimally.

Y. G. Li thanks the Chinese Scholarship Council (CSC), while A. De Sarkar, B. Pathak and R. Ahuja would like to gratefully acknowledge the funding support from the Wenner-Gren Stiftelserna/Foundation. R.A. also thanks FORMAS, STEM and SWECO, Sweden. SNIC and UPPMAX are acknowledged for computing time.

[1]L. Dai and A. W. H. Mau, Adv. Mater. **13**(12-13), 899–913 (2001).
[2]B. Panella, M. Hirscher, and S. Roth, Carbon **43**(10), 2209–2214 (2005).
[3]Z. Sun, H. Yuan, Z. Liu, B. Han, and X. Zhang, Adv. Mater. **17**(24), 2993–2997 (2005).
[4]A. Kaniyoor, R. Imran Jafri, T. Arockiadoss, and S. Ramaprabhu, Nanoscale **1**(3), 382–386 (2009).
[5]N. A. Kaskhedikar and J. Maier, Adv. Mater. **21**(25–26), 2664–2680 (2009).
[6]M. Zhou, Y. Lu, C. Zhang, and Y. P. Feng, Appl. Phys. Lett. **97**(10), 103109 (2010).
[7]L. Wang, K. Lee, Y.-Y. Sun, M. Lucking, Z. Chen, J. J. Zhao, and S. B. Zhang, ACS Nano **3**(10), 2995–3000 (2009).
[8]Y. Shao, J. Wang, H. Wu, J. Liu, I. A. Aksay, and Y. Lin, Electroanalysis **22**(10), 1027–1036 (2010).
[9]C. Ataca, E. Akturk, S. Ciraci, and H. Ustunel, Appl. Phys. Lett. **93**(4), 043123–043125 (2008).
[10]D. Cao, J. Lan, W. Wang, and B. Smit, Angew. Chem. **121**(26), 4824–4827 (2009).
[11]E. Durgun, S. Ciraci, W. Zhou, and T. Yildirim, Phys. Rev. Lett. **97**(22), 226102 (2006).
[12]C. J. Doonan, D. J. Tranchemontagne, T. G. Glover, J. R. Hunt, and O. M. Yaghi, Nat. Chem. **2**(3), 235–238 (2010).
[13]C. Li, J. Li, F. Wu, S.-S. Li, J.-B. Xia, and L.-W. Wang, J. Phys. Chem. C **115**(46), 23221–23225 (2011).
[14]M. Yoon, S. Yang, C. Hicke, E. Wang, D. Geohegan, and Z. Zhang, Phys. Rev. Lett. **100**(20), 206806 (2008).
[15]Q. Sun, P. Jena, Q. Wang, and M. Marquez, J. Am. Chem. Soc. **128**(30), 9741–9745 (2006).
[16]C. Cazorla, S. A. Shevlin, and Z. X. Guo, Phys. Rev. B **82**(15), 155454 (2010).
[17]T. Hussain, A. De Sarkar, and R. Ahuja, Appl. Phys. Lett. **101**(10), 103907 (2012).
[18]S. M. Lee, K. H. An, Y. H. Lee, G. Seifert, and T. Frauenheim, J. Am. Chem. Soc. **123**(21), 5059–5063 (2001).
[19]S. A. Shevlin and Z. X. Guo, J. Phys. Chem. C **112**(44), 17456–17464 (2008).
[20]G. Kim, S.-H. Jhi, S. Lim, and N. Park, Phys. Rev. B: Condens. Matter **79**(15), 155437 (2009).
[21]K. S. Kim, Y. Zhao, H. Jang, S. Y. Lee, J. M. Kim, K. S. Kim, J.-H. Ahn, P. Kim, J.-Y. Choi, and B. H. Hong, Nature **457**(7230), 706–710 (2009).
[22]C. Lee, X. Wei, J. W. Kysar, and J. Hone, Science **321**, 385–388 (2008).
[23]J. Zhou, Q. Wang, Q. Sun, P. Jena, and X. S. Chen, PNAS **107**, 2801–2806 (2010).
[24]C.-S. Liu and Z. Zeng, Appl. Phys. Lett. **96**(12), 123101 (2010).
[25]D. W. Boukhvalov and M. I. Katsnelson, J. Am. Chem. Soc. **130**(32), 10697–10701 (2008).
[26]I. Jung, D. A. Dikin, R. D. Piner, and R. S. Ruoff, Nano Lett. **8**(12), 4283–4287 (2008).
[27]M. Seredych and T. J. Bandosz, J. Colloid Interface Sci. **324**(1), 25–35 (2008).
[28]K. A. Mkhoyan, A. W. Contryman, J. Silcox, D. A. Stewart, G. Eda, C. Mattevi, S. Miller, and M. Chhowalla, Nano Lett. **9**(3), 1058–1063 (2009).
[29]O. C. Compton and S. T. Nguyen, Small **6**(6), 711–723 (2010).
[30]Y. Zhu, S. Murali, W. Cai, X. Li, J. W. Suk, J. R. Potts, and R. S. Ruoff, Adv. Mater. **22**(35), 3906–3924 (2010).
[31]T.-F. Yeh, F.-F. Chan, C.-T. Hsieh, and H. Teng, J. Phys. Chem. C **115**(45), 22587–22597 (2011).
[32]W. S. Hummers and R. E. Offeman, J. Am. Chem. Soc. **80**(6), 1339 (1958).
[33]J. Dai, J. Yuan, and P. Giannozzi, Appl. Phys. Lett. **95**(23), 232105 (2009).
[34]G. Kresse and D. Joubert, Phys. Rev. B: Condens. Matter **59**(3), 1758–1775 (1999).
[35]J. P. Perdew, K. Burke, and M. Ernzerhof, Phys. Rev. Lett. **77**(18), 3865–3868 (1996).
[36]P. E. Blöchl, Phys. Rev. B: Condens. Matter **50**(24), 17953–17979 (1994).
[37]J. D. Pack and H. J. Monkhorst, Phys. Rev. B: Condens. Matter **16**(4), 1748–1749 (1977).
[38]C. Kittel and P. McEuen, *Introduction to Solid State Physics* (Wiley New York, 1996).
[39]Z. Fan, K. Wang, T. Wei, J. Yan, L. Song, and B. Shao, Carbon **48**(5), 1686–1689 (2010).
[40]S. Grimme, J. Comput. Chem. **27**, 1787–1799 (2006).